Engineering Structures 111 (2016) 323–332

Contents lists available at ScienceDirect

Engineering Structures

journal homepage: www.elsevier.com/locate/engstruct

Shear strength of steel fibre reinforced concrete beams with stirrups

Ali Amin [a,*], Stephen J. Foster [b]

[a] Centre for Infrastructure Engineering and Safety, School of Civil and Environmental Engineering, The University of New South Wales, Australia
[b] School Civil and Environmental Engineering, The University of New South Wales, Australia

ARTICLE INFO

Article history:
Received 29 July 2015
Revised 16 December 2015
Accepted 17 December 2015

Keywords:
Steel fibre
Shear
Concrete
Stirrups

ABSTRACT

Despite the increased awareness of Steel Fibre Reinforced Concrete (SFRC) in practice and research, SFRC is yet to find common application in load bearing or shear critical building structural elements. Although the far majority of studies on SFRC have focused on members containing fibres only, in most practical applications of SFRC construction, structural members made of SFRC are also reinforced with conventional reinforcing steel for shear ligatures. In this paper, results are presented on shear tests which have been conducted on ten 5 m long by 0.3 m wide by 0.7 m high rectangular simply supported beams with varying transverse and steel fibre reinforcement ratios. The tests have been analysed along with complete material characterisation which quantify the post-cracking behaviour of the SFRC. A procedure based on the model proposed by Foster (2010) is presented alongside predictions from the *fib* Model Code 2010 (Final Draft, 2012) and Draft Australian Bridge Code: Concrete (DR AS5100.5, 2014) and is shown to correlate well with the test data.

1. Introduction

Research into the use of steel fibres as tensile and shear reinforcement in concrete has been underway for more than five decades [1]. Experimental investigations have shown that the inclusion of steel fibres in concrete, when adopted in ample quantities, improves the shear resistance of beams by increasing the tensile and post-cracking or energy absorption characteristics of the concrete. Steel fibres can delay the formation and propagation of cracks by improving the effectiveness of the crack-arresting mechanisms present in beams when applied under high shear stresses.

Many studies have considered the possibility of utilising SFRC by assigning a proportion of the shear resisting capacity of beams to the fibres. This concept has been realised by ACI-318 [2], and more recently by the *fib* Model Code 2010 [3] and the Draft Australian Bridge Code for Concrete Structures DR AS5100.5 [4].

Despite the increased awareness in practice and research, SFRC is yet to find common application in load bearing building structural elements. SFRC has largely been limited to use in non-critical members, even though significant potential exists for full or partial replacement of costly, manually placed, shear reinforcement (links/stirrups).

In examining the research on the shear behaviour and strength of SFRC beams, most studies have focused on members containing fibres only as shear reinforcement [5–11], with few studies on the shear capacity of SFRC combined with conventional reinforcing steel for shear ligatures [12–15]. Moreover, a study of these beams within the literature reveals that most of the members tested actually failed in flexure, not shear. In this context, this paper reports an experimental program intended to investigate the response of large scale SFRC beams co-reinforced with stirrups and designed to fail in shear.

2. Experimental investigation

An experimental program was conducted to investigate the combined effect of steel fibres and traditional transverse reinforcement on the response of beams subjected to four-point loading. Ten large-scale beams with various fibre volumes and transverse reinforcement ratios were constructed and tested to failure. As the investigation was designed for the specimens to fail in shear, the beams were reinforced to ensure that flexural tensile failure did not occur.

The specimens were designated using the notation *BW-X-Y-Z* where '*W*' is the dosage of steel fibres (in kg/m^3), '*X*' is the stirrup steel strength grade (in MPa), '*Y*' is the diameter of stirrups (in mm) and '*Z*' is the stirrup spacing (in mm) within the critical shear regions. For example, specimen B25-550-6-450 represents a beam

* Corresponding author. Tel.: +61 2 9385 5033.
E-mail address: Ali.Amin@unsw.edu.au (A. Amin).

http://dx.doi.org/10.1016/j.engstruct.2015.12.026
0141-0296/

reinforced with 25 kg/m^3 of steel fibres and 6 mm grade 550 MPa stirrups spaced at 450 mm c/c within the critical shear regions.

The specimen dimensions and testing arrangements are shown in Fig. 1. The beams had an overall depth of 700 mm, were 300 mm wide and 5000 mm long. The shear span to effective depth ratio (a/d_e) was chosen as 2.8, to reduce any effects due to arching [16], resulting in a shear span of 1750 mm and a constant moment region of 1000 mm. The clear concrete cover was 25 mm. One end of each specimen was pinned supported and the other end had a roller support. The pin and the roller were greased to minimise friction and to give free rotation and horizontal translation, as required. To avoid crushing at the supports and loading points, the loads and reactions were applied through 200 mm by 350 mm by 20 mm thick steel plates.

The longitudinal reinforcement was fabricated from Class N nominally 500 MPa grade, hot rolled, deformed bars. The beams contained two layers of three normal ductility 28 mm diameter tensile reinforcement (N28), which corresponds to a flexural reinforcement ratio of 0.0198. Two 20 mm diameter longitudinal reinforcing bars (N20) were located at the top section of the beam. The stress strain relations for the reinforcing steel are shown in Fig. 2. The yield strength of the N20 and N28 bars were 560 MPa and 540 MPa, respectively, the ultimate strengths were 650 MPa and 640 MPa, respectively and the strains at the end of uniform elongation were 10.9% and 11.3%, respectively (refer to Fig. 2a). The tensile longitudinal reinforcement bars were cogged upwards at their ends beyond the supports to provide mechanical anchorage for the bars.

Four grades of shear ligatures (stirrups) were used in this study. They were fabricated from nominal 550 MPa, 450 MPa, 400 MPa or 300 MPa drawn wire reinforcement; the measured yield strengths are presented in Fig. 1 and the stress–strain curves in Fig. 2b. The transverse reinforcement was detailed in accordance with the minimum shear provisions of AS3600 [17] and EC-2 [18], resulting in a stirrup spacing of 300 mm and 450 mm, respectively.

The steel fibres used in this study were the structural grade double end-hooked Dramix®5D-65/60-BG fibre. The fibres were 0.9 mm in diameter and 60 mm long. The fibres are characterised by an ultimate notional tensile strength of 2300 MPa and increased anchorage within a concrete matrix. Two fibre dosages were used in this study; the minimum fibre dosage was designed by equating the shear resistance provided by the minimum required shear reinforcing prescribed by the *fib* Model Code 2010 [3] to an equivalent dosage of fibres. The dosage was quantified using the predicative tensile constitutive law described by the Variable Engagement Model (VEM) [19,20] at an ultimate crack width of 1.50 mm. This resulted in a fibre dosage of 25 kg/m^3. A second fibre dosage of 50 kg/m^3 was adopted for three beams to assess the influence of fibre volume to the shear resistance of the SFRC beams. It is noted that a fibre dosage of 25 kg/m^3 just falls within structural guidelines such as CNR DT 204/2006 [21] for the minimum volume of fibres in SFRC.

The SFRC beams were manufactured over three separate pours. The concrete was provided to the testing laboratory without the fibres in the mix; the specified target concrete compressive strength was 32 MPa. The first pour comprised of beams B0-450-10-450, B25-0-0-0, B25-550-6-450 & B25-450-10-450; the second pour beams B25-400-6-300 & B25-300-10-300; the third pour beams B0-550-6-450, B50-0-0-0, B50-550-6-450 & B50-450-10-450 (refer to Fig. 1). For the pours that had specimens without

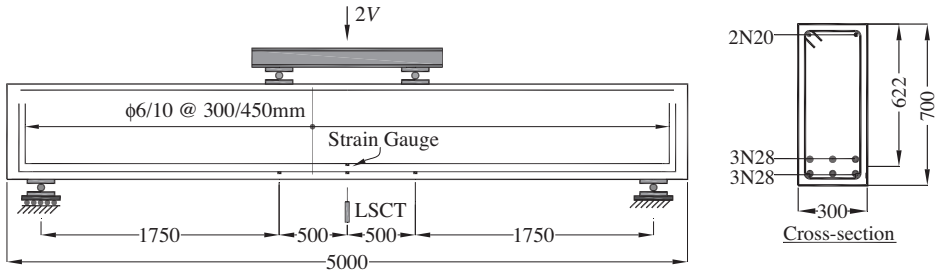

Beam ID	Pour	Measured Fibre Dosage: Mean (St. Dev) kg/m^3	f_{cm} (MPa)	E_c (GPa)	Transverse Reinforcement	Transverse Steel Yield Strength (MPa)
B0-450-10-450	1	0	34	28	2 leg R10 @ 450mm	447
B25-0-0-0	1	25.0 (0.5)	34	28	-	-
B25-550-6-450	1	25.0 (0.5)	34	28	2 leg R6 @ 450mm	553
B25-450-10-450	1	25.0 (0.5)	34	28	2 leg R10 @ 450mm	447
B25-400-6-300	2	23.0 (4.6)	46	37	2 leg R6 @ 300mm	402
B25-300-10-300	2	23.0 (4.6)	46	37	2 leg R10 @ 300mm	277
B0-550-6-450	3	0	36	43	2 leg R6 @ 450mm	553
B50-0-0-0	3	53.6 (10.2)	36	43	-	-
B50-550-6-450	3	53.6 (10.2)	36	43	2 leg R6 @ 450mm	553
B50-450-10-450	3	53.6 (10.2)	36	43	2 leg R10 @ 450mm	447

Fig. 1. Experimental arrangement (mm) and specimen details.

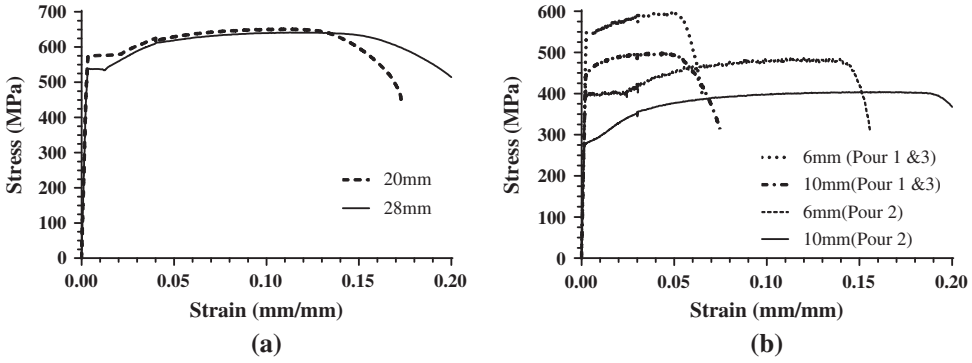

Fig. 2. Stress vs strain relationship for (a) longitudinal reinforcement; (b) transverse reinforcement.

fibres, these specimens were cast first. The calculated weight of the fibres was then added, on-site, and mixed in the agitator for a minimum of 10 min; when fully mixed, the SFRC specimens were cast.

For each pour, after the fibres were added in the agitator, the actual fibre content was determined by extracting three cylinders (150 mm diameter by 300 mm high) at the start of the pour and a further three cylinders at the end of the pour. The cylinders were emptied the cement content washed out and the fibres extracted using a magnet. The fibres were then dried and their weight measured. The average fibre dosages, and standard deviations, are given in Fig. 1.

All beam specimens were tested in an Instron 5000 kN stiff testing frame and tested under a ram displacement control of 0.3 mm/min. A linear strain conversion transducer (LSCT) was placed at the beam mid-span to measure displacement (see Fig. 1). All beams were instrumented with electrical resistance strain gauges bonded to the reinforcing bars before casting. The strain gauges were placed on the lower tensile reinforcing layer at mid-span and under the load points as well as on the upper tensile reinforcing layer at mid-span only (Fig. 1) to verify that failure of the beams was one of shear. The front and back surfaces of the beams were painted white and a 100 mm × 100 mm grid was drawn on to the front surface to aid in the monitoring of the development and propagation of cracks during testing.

3. Mechanical properties of SFRC

To characterise the performance of the SFRC beams, it is necessary to ascertain the post cracking or residual strength of the material. The measured short term mechanical properties of the SFRC are presented in Figs. 3 and 4. The fracture properties of the SFRC were determined directly by obtaining the tensile strength of the concrete matrix, f_{ct}, and the average residual tensile strength, $f_{1.5}$ (taken at a crack width of 1.5 mm), from six uniaxial 'dogbone' specimens (Fig. 4a) tested to [4]. The tensile properties were also determined indirectly from the residual flexural strength, $f_{R,j}$, through six three-point notched prisms tested to [22]. The mean compressive strength, f_{cm}, and Young's modulus, E_c, at the day of beam testing were determined by testing three 150 mm diameter × 300 mm high cylinders. It is noted that the results presented in Fig. 4 have been compensated for the boundary/wall effect [23]; that is, the presence of a boundary (or in the case of the uniaxial tension test specimens, the wall) restricts a fibre from being freely orientated in space. An orientation factor must be applied to the raw experimental results to convert them to an equivalent 3D distribution free of boundary influences. For the fibres used in this study (l_f = 60 mm); the orientation factor is calculated as k_t = 0.81, in accordance with [4].

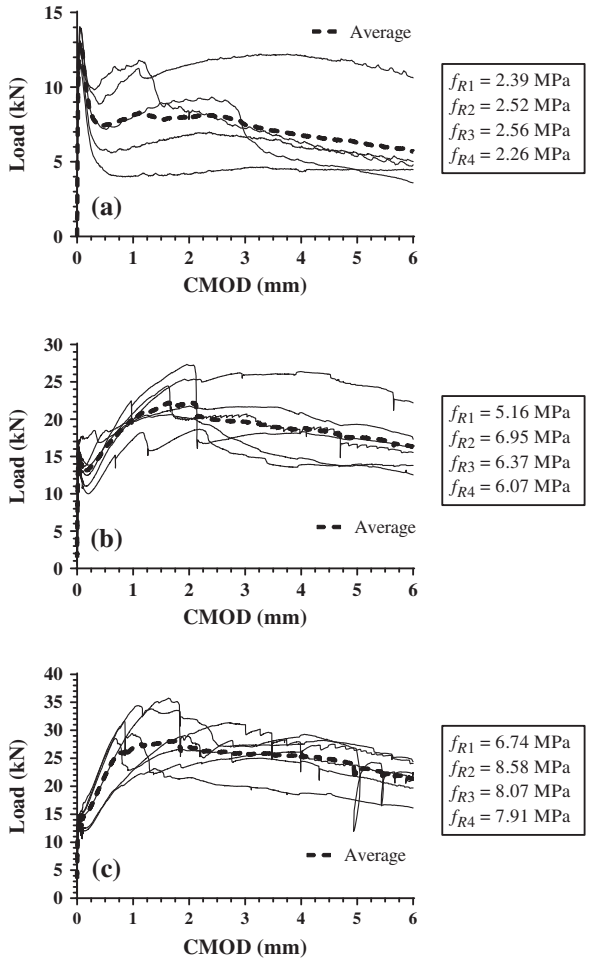

Fig. 3. Three point prism bending test results: (a) Pour 1; (b) Pour 2; (c) Pour 3.

4. Beam test results

A comparison of the shear versus mid-span deflection responses for the beam specimens are presented in Fig. 5. Table 1 compares the values for the observed cracking shear, V_{cr}; maximum shear capacity, $V_{u,test}$; the maximum applied shear stress, v_u; the deflection at peak load, δ_u; the average maximum strain in the longitudinal tensile reinforcement obtained from the strain gauges at the bottom layer of the mid span, ε_s; the measured angle of inclination of the critical shear crack at beam mid-height, θ_{exp}; and the ratio between the maximum applied moment, M_a, to its flexural capacity, M_u (as determined from

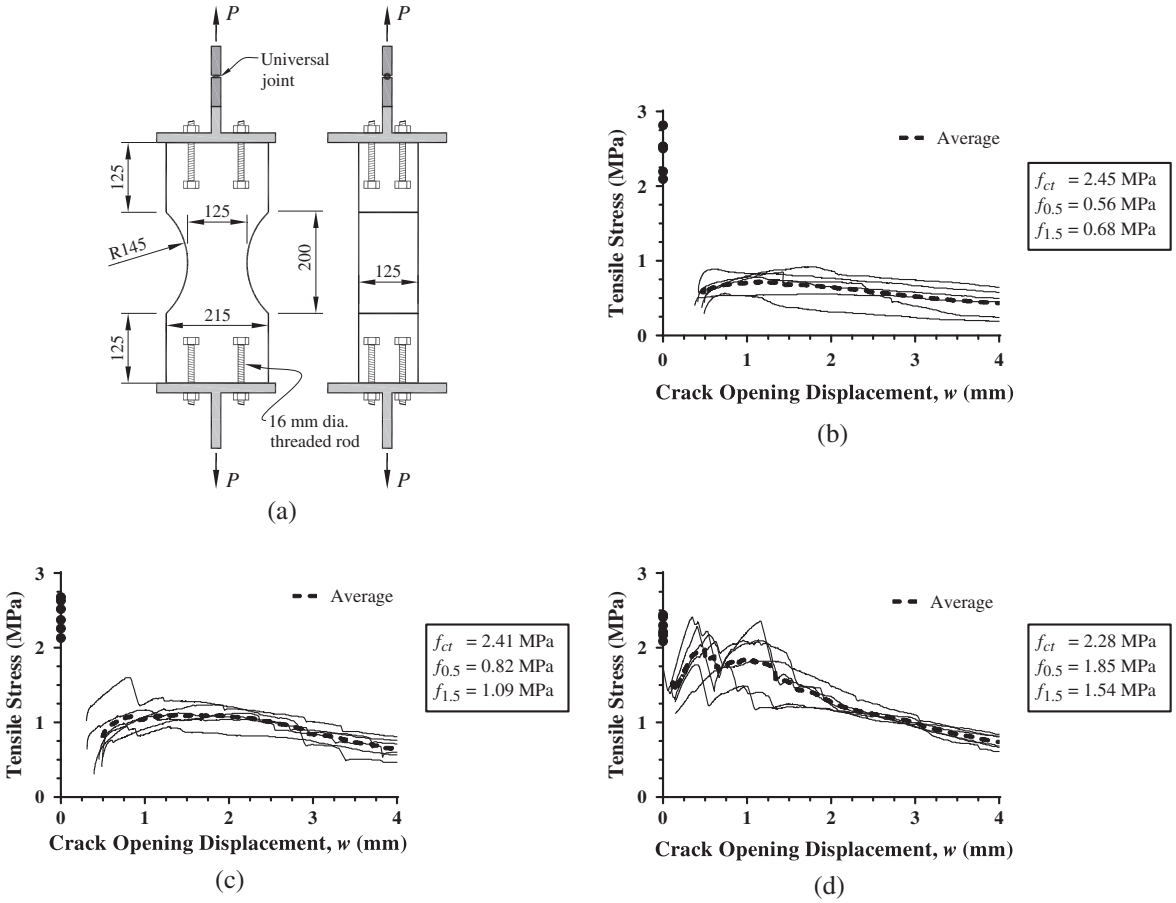

Fig. 4. Uniaxial tension test: (a) details; results (b) Pour 1; (c) Pour 2; (d) Pour 3.

[4]). All beams have been compensated for the minimal support displacements that were measured.

With the exception of specimen B50-450-10-450, the bottom layer of tensile reinforcing steel in all specimens remained below their yielding value ($\varepsilon_s < \varepsilon_{sy}$) and failure of the specimens was that of shear. For specimen B50-450-10-450, the maximum strain was slightly above yield but well below ultimate. The observed shear cracking load, V_{cr}, was relatively insensitive to the total shear reinforcement.

A comparison of the crack patterns (Fig. 6) show all the beams which failed in shear to have behaved in a similar manner with distinguished inclined shear cracks initiating in the centre of the shear spans. The observed formation of diagonal shear cracks occurred at V_{cr}. The diagonal cracks propagated from the mid-height of the beams towards the loading points with increasing load. Finally, failure of the beam resulted from fracture across a single, dominant crack or from a coalescence of cracks leading to the formation of a dominant crack, or, interestingly, in the case of B25-0-0-0, the formation of two parallel dominant cracks. In general, the addition of fibres led to an increase in the number of cracks and a reduction in observed crack widths to form a more diffused crack pattern. The rate of crack growth was dependant on the fibre dosage- the cracks propagated more slowly in the beams with higher fibre dosages.

A comparison of the shear capacities of B0-450-10-450 and B25-0-0-0 verified that a fibre dosage of 25 kg/m^3 represents an equivalent dosage to the minimum transverse reinforcement required by [18]. Examining the post peak behaviour of these beams shows that while the specimen containing only fibres reached a higher ultimate strength, the subsequent reduction in load after failure was more rapid (i.e. more brittle). A close inspection of all the beams with stirrups showed that the stirrups crossing the dominant crack had not fractured.

Comparing the maximum peak load of beams B25-450-10-450 and B25-550-6-450 indicates that the specimen with larger stirrups failed at a lower peak load than that of specimen B25-550-6-450. An examination of the specimens after testing showed that the dominant shear crack engaged only one stirrup in beam B25-450-10-450 but had engaged two stirrups in beam B25-550-6-450. This unexpected result is attributed to the normal variability of the material; an important aspect which must be considered when designing concrete beams reinforced with fibres for shear. Examining the specimens with reduced stirrup spacing shows that although lower cracking shear loads (V_{cr}) were observed, larger deflections were sustained at the peak load and the post-peak response was more ductile.

Specimen B50-0-0-0 had an ultimate shear capacity of 344 kN with damage occurring in one shear span only (refer to Fig. 6h). During the test, only one hairline shear crack was visible in the other shear span, which appeared at an applied shear of 185 kN. After completion of the test, the failed shear span was strengthened using an external yoke system and retested (see Fig. 7). The retested specimen (B50-0-0-0R) was then loaded in the same manner until failure. The ultimate shear capacity of the retested shear span was 409 kN, 19% greater than obtained in the original test. This demonstrates the variability that is expected in testing of reinforced concrete beams in shear.

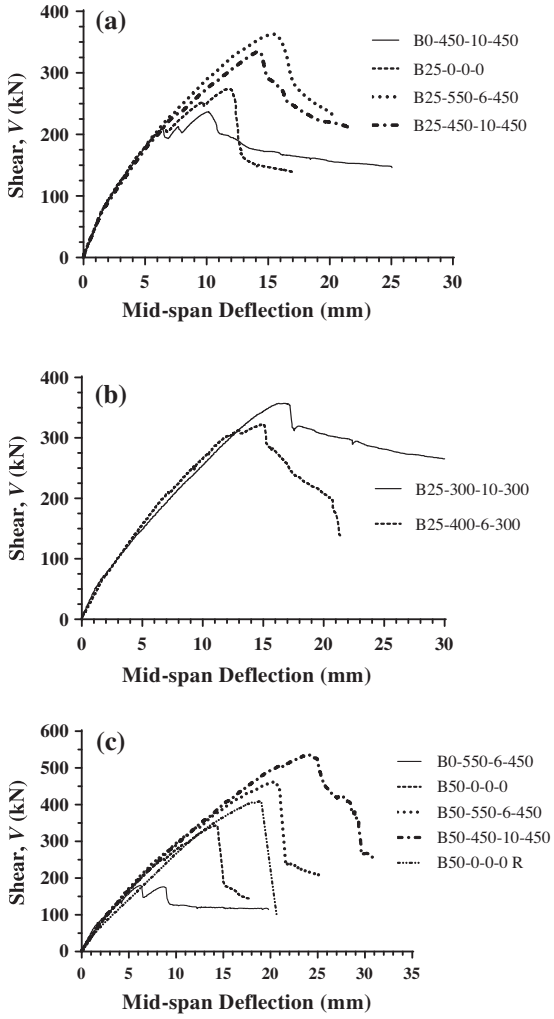

Fig. 5. Comparison of shear versus mid-span deflection responses: (a) Pour 1; (b) Pour 2; (c) Pour 3.

5. Design guidelines for the shear resistance of SFRC beams

In this section, a comparison is undertaken between the ultimate shear capacity obtained by the experimental investigation and predicted values from expressions proposed in national codes and in the literature. Although there has been significant research effort into quantifying the shear behaviour of SFRC beams, the majority of models proposed are empirical in nature and rely on regression analysis for some parameters [24]. Generally, design models take the total shear, V_u, to be resisted partially by a component taken by the concrete, V_{uc}, a component taken by the transverse steel ligature reinforcement, V_{us}, and a component taken by the fibres, V_{uf}. The V_{uc} component is taken as the shear at the commencement of diagonal cracking and is often determined empirically. V_{us} can be obtained from a truss model.

5.1. *fib* Model Code 2010 [3]

The *fib* Model Code 2010 recommended that the shear resistance, V_u, be calculated by:

$$V_u = V_{us} + V_R \tag{1}$$

where V_{us} is the design shear strength taken by the transverse reinforcement and V_R is the design shear strength contributed by the matrix and fibres ($V_R = V_{uc} + V_{uf}$). For non prestressed elements, V_R is:

$$V_R = \frac{0.18kbd_e}{\gamma_c}\left(100\rho f_{cm}\left(1 + 7.5\frac{f_{Ftu}}{f_{ct}}\right)\right)^{1/3} \tag{2}$$

where γ_c is the partial safety factor for concrete, ρ_l is the tensile longitudinal reinforcement ratio, f_{Ftu} is the ultimate residual flexural-tensile strength for SFRC, corresponding to an ultimate crack width, w_u = 1.5 mm (as prescribed in [3]) and can be taken as:

$$f_{Ftu} = 0.30f_{R3} + 0.06f_{R1} \tag{3}$$

In Eq. (2), b is the width of the web, d_e is the effective depth of the section and k is the size effect parameter:

$$k = 1 + \sqrt{200/d_e} \leqslant 2 \tag{4}$$

In this paper this model is referred to as the MC1 model. A close examination of Eq. (2) reveals that the fibre component is treated as additional longitudinal reinforcement smeared over the cross section of the beam and is adapted to the context of the Eurocode 2 [18] model for shear in reinforced concrete beams. For further information on the derivation of this model, the reader is referred to [7].

5.2. Foster [25]

Foster [25] developed a shear model for SFRC beams based on the simplified modified compression field theory (MCFT) of Bentz et al. [26]. The model was developed to calculate the critical section for shear and assumed a uniform shear stress distribution throughout the depth of the member and features as the alternative model for shear in the *fib* Model Code 2010 [3]. In this paper this model is notated as the MC2 model. The model assumes that the contribution of the fibres and concrete matrix are coupled, as each is a function of the critical crack width and, therefore, must be solved simultaneously. In this study the capacity of the stirrups, V_{us}, is included in the iterative process (Fig. 8) [27]. The concrete

Table 1
Summary of beam test results.

Beam ID	V_{cr} (kN)	$V_{u,test}$ (kN)	v_u (MPa)	δ_u (mm)	ε_s (με)	θ_{exp}	M_a/M_u
B0-450-10-450	200	236	1.26	10.1	1262	43	0.37
B25-0-0-0	190	274	1.47	11.8	1668	30	0.44
B25-550-6-450	200	363	1.93	15.3	1935	50	0.59
B25-450-10-450	200	334	1.79	14.2	1831	41	0.54
B25-400-6-300	180	322	1.71	15.0	1613	53	0.48
B25-300-10-300	155	357	1.91	16.6	2040	42	0.54
B0-550-6-450	170	180	0.96	6.2	1059	32	0.28
B50-0-0-0	180	344	1.84	14.3	1691	31	0.52
B50-0-0-0R	185	409	2.19	18.8	–	52	0.62
B50-550-6-450	230	462	2.46	20.5	2651	29	0.70
B50-450-10-450	220	535	2.87	24.2	2753	42	0.81

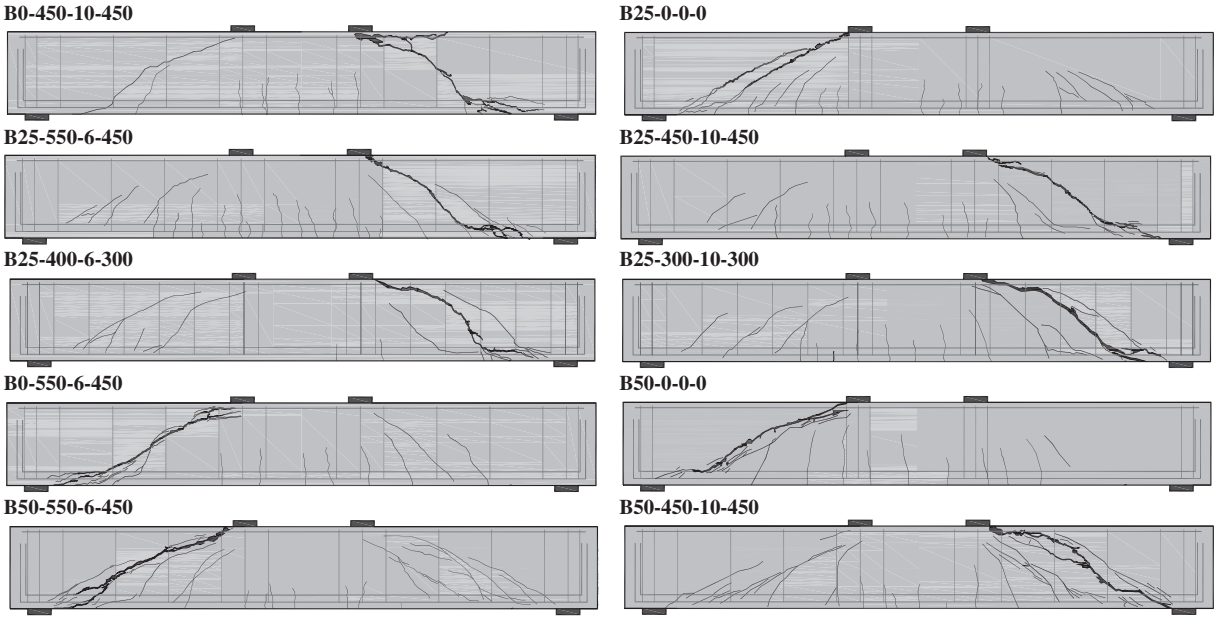

Fig. 6. Crack patterns at failure.

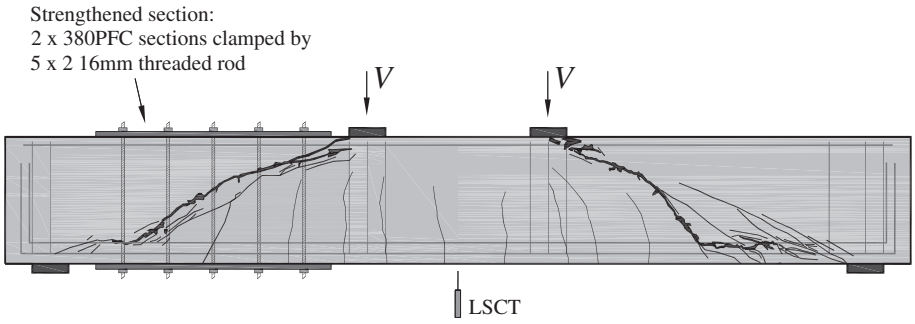

Fig. 7. Test setup and crack pattern at failure Beam B50-0-0-0R.

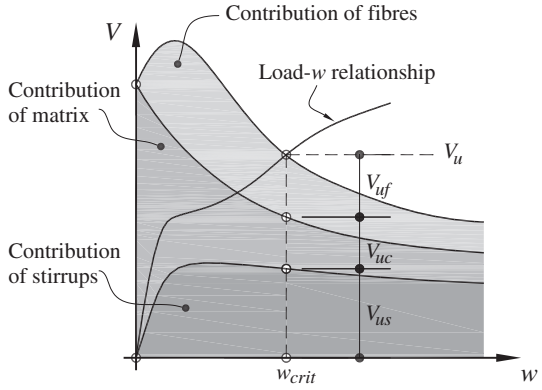

Fig. 8. Coupling of matrix and transverse reinforcement with fibre component for the determination of the shear capacity of SFRC beams with stirrups [27].

and non-inclined stirrup shear components are based on the Level III model of the *fib* Model Code 2010 [3] and taken, respectively, as:

$$V_{uc} = k_v \sqrt{f_{cm}} bz \tag{5}$$

$$V_{us} = \frac{A_{sv}}{s_w} f_{sy,f} z \cot\theta \tag{6}$$

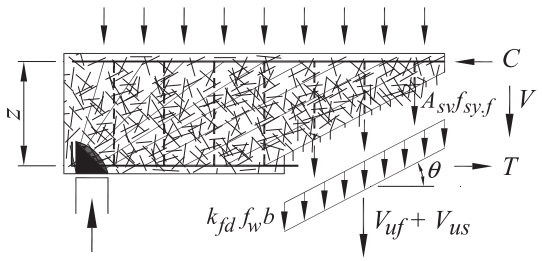

Fig. 9. Transverse and fibre reinforcing components of SFRC beams with stirrups failing in shear [25].

where A_{sv} and s_w are the cross sectional area and spacing of the shear reinforcement, respectively and $f_{sy,f}$ is the design strength of the transverse reinforcement. The internal flexural lever arm between the centroids of the flexural tensile and compressive stress resultants, z, can be approximated as $0.9d_e$ (see Fig. 9).

The strain-aggregate size parameter, k_v, is derived from the MCFT and determines the capacity of the section to resist aggregate interlock:

$$k_v = \frac{0.4}{1 + 1500\varepsilon_x} \times \frac{1300}{1000 + k_{dg} z} \tag{7}$$

The first term of Eq. (7) models the strain effect and is based on a linear approximation of the crack width relationship to the longitudinal strain at mid-depth of the member. It is shown in [26] that this term gives an indication of the ability of the cracked concrete to transfer shear stresses across cracks. The second term of Eq. (7) models the size effect. The parameter k_{dg} is a function of the maximum aggregate size and is taken as:

$$k_{dg} = \frac{32}{16 + d_g} \geqslant 0.75 \tag{8}$$

For light weight and high strength concrete ($f_{cm} > 70$ MPa), cracks tend to pass through the aggregate, as opposed to around them, leading to smoother crack surfaces with less aggregate interlock capacity. In these cases d_g is taken as zero.

The crack widths that govern the aggregate interlock capacity and the contribution of the fibres in resisting tension can be related to the longitudinal strain at mid-height, ε_x. This strain can be calculated by determining the average longitudinal strains in the flexural tension and flexural compression regions of the member. A suitably conservative expression for ε_x is taken as half of the tensile strain in the flexural tensile reinforcement, assuming that the member contains only concentrated longitudinal reinforcement:

$$\varepsilon_x = \frac{M/z + 0.5V\cot\theta}{2E_sA_s} \tag{9}$$

In Eq. (9) M and V correspond to the moment and shear, respectively, at the critical section and E_s and A_s are the elastic modulus and area of the longitudinal steel, respectively. The crack width at the mid-height on the section, w, can be taken as [28]:

$$w = 0.2 + 1000\varepsilon_x \geqslant 0.125 \text{ mm} \tag{10}$$

The MCFT predicts the angle of the principal compressive stress, or strut angle θ, at shear failure for members with shear reinforcement to depend primarily upon the longitudinal strain ε_x. The angle θ is determined as:

$$\theta = 29^\circ + 7000\varepsilon_x \tag{11}$$

The steel fibres contribution to the shear strength (Fig. 10) is a function of the critical crack width and, hence, the longitudinal strain. The fibre contribution averaged over the failure surface is:

$$V_{uf} = k_{fd}f_w bz\cot\theta \tag{12}$$

In Eq. (12), k_{fd} is a fibre dispersion reduction factor, taken as $k_{fd} = 0.82$. The factor represents the average stress factor for a critical crack forming along the path of least resistance as explained in Foster [25]. The tensile strength provided by the steel fibres over a plane of unit area, f_w, can be obtained from the uniaxial tension test data. In the absence of direct test data and presence of suitable prism bending data, an inverse analysis procedure such as that reported in [23,29] can be used to convert force–displacement data to a representative stress versus COD state.

An iterative method is required to solve for the shear capacity of the SFRC beam as ε_x is required in the calculation of both the fibre and concrete contribution at the critical section. In predicting the failure load of the beam, it is necessary to also consider other failure modes, for example flexure. The advantage of this model is that it is able to unify the design of SFRC beams with and without traditional steel shear ligature reinforcement within the same framework.

5.3. DR AS5100.5 [4]

To overcome the combined iterative process of the *fib* MC2 model, a simplified adaptation to the model is incorporated in the Draft Australian Bridge Code DR AS5100.5: Concrete, in which a level I approximation is used. The shear strength is given by:

$$V_u = V_{uc} + V_{us} + V_{uf} \tag{13}$$

$$V_{uf} = 0.7k_\theta bdf_{1.5} \tag{14}$$

where $k_\theta = \cot\theta \leqslant 1.28$. The components V_{uc} and V_{us} are determined from Eqs. (5) and (6).In quantifying the component of shear resisted by the ligatures, the location of the critical shear crack can have a large impact on the calculated capacity of the section, particularly if the number of stirrups passing through the critical shear crack is low. Loov [30] considered the crack patterns illustrated in Fig. 10. If the critical shear crack initiates between stirrups, (Fig. 10(a)) the number of engaged stirrups that cross the crack is equal to $z\cot\theta/s_w$. On the other hand, if the crack initiates besides a stirrup, and is unable to effectively engage the stirrup (Fig. 10 (b)), the number of effective stirrups crossing the crack is equal to $z\cot\theta/s_w - 1$. The situation described in Fig. 10b usually occurs more frequently as bar chairs or flaws under the stirrup reinforcement act as crack initiators. It is for this reason that code equations for V_{us} occasionally overestimate the contribution provided by the ligatures.

The results obtained from the three models introduced above are compared to the experimental results, $V_{u,test}$, in Tables 2 and 3 with $\gamma_c = 1$. In Tables 2 and 3, three results are presented for the code analyses. In the left column, V_{us} is taken as $nA_{sw}f_{sy,f}$ where n is the number of stirrups that were actually crossed by the shear crack, as observed in the experiments. In the middle column, the values shown are those predicted with the stirrups taken as smeared along the member ($n = z\cot\theta/s_w$); and in the right column, the number of stirrups crossing the crack is taken as $n = \lfloor z\cot\theta/s_w \rfloor$, noting that the number of stirrups crossing a crack must be an integer value. It is noted that adopting $n = \lfloor z\cot\theta/s_w \rfloor - 1$ would grossly underestimate the contribution of the stirrups, particularly when the ligatures are widely spaced; this become less significant as the number of stirrups intersecting the crack increases. For the determination of f_w in Eq. (12), the average stress of the six uniaxial tension tests (see Fig. 4a) is computed for the theoretical critical shear crack width (w) taken at the mid-height of the section.

The results indicate that the *fib* MC2 and DR AS5100.5 models adequately predict the shear capacity of the beams; provided the number of stirrups is adjusted for the case where crack initiation is adjacent to the stirrup. The *fib* MC1 model tends to slightly over predict the shear capacity of the beams.

The MC2 model is further assessed against experimental results reported in the literature for which material data (prism bending tests) exists and the failure mode of the beams was one of shear without the longitudinal bars reaching yield. The tests include

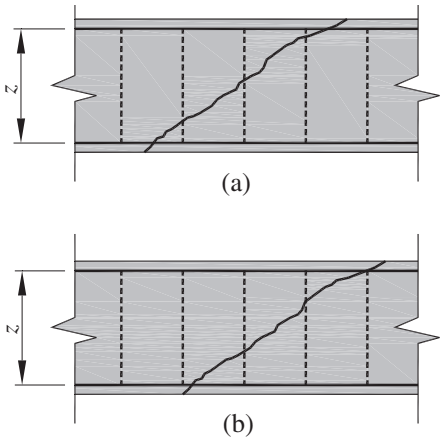

Fig. 10. Number of stirrups crossing critical shear crack [30].

Table 2
Predictions of shear resistance.

Beam ID	n	$V_{u,test}$ (kN)	$V_{fib\ MC1}$ (kN)			$V_{fib\ MC2}$ (kN)			$V_{DR\ AS\ 5100.5}$ (kN)		
			With n	Smeared	Integer	With n	Smeared	Integer	With n	Smeared	Integer
B0-450-10-450	1	236	231	297	280	231	297	280	242	310	242
B25-0-0-0	0	274	334	334	334	284	284	284	241	241	241
B25-550-6-450	2	363	397	412	397	333	328	308	348	347	317
B25-450-10-450	1	334	404	496	474	339	380	339	355	424	355
B25-400-6-300	1	322	484	544	530	373	400	391	396	440	396
B25-300-10-300	2	357	548	610	592	424	439	424	460	500	417
B0–550-6-450	1	180	209	240	230	209	240	230	207	237	207
B50-0-0-0	0	344	474	474	474	424	424	424	432	432	432
B50-0-0-0R	0	409	474	474	474	424	424	424	432	432	432
B50-550-6-450	2	462	537	552	537	457	453	462	496	495	464
B50-450-10-450	2	535	615	636	615	512	494	535	573	571	503

Table 3
Predictions of shear resistance compared to experimental data.

Beam ID	$\frac{V_{u,test}}{V_{fib\ MC1}}$			$\frac{V_{u,\ test}}{V_{fib\ MC2}}$			$\frac{V_{u,\ test}}{V_{DR\ AS5100.5}}$		
	With n	Smeared	Integer	With n	Smeared	Integer	With n	Smeared	Integer
B0-450-10-450	1.02	0.79(2.31)	0.84(2)	1.02	0.79(2.31)	0.84(2)	0.98	0.76(1.98)	0.98(1)
B25-0-0-0	0.82	0.82(0)	0.82(0)	0.96	0.96(0)	0.96(0)	1.14	1.14(0)	1.14(0)
B25-550-6-450	0.91	0.88(2.43)	0.91(2)	1.09	1.11(1.78)	1.18(1)	1.04	1.05(1.98)	1.15(1)
B25-450-10-450	0.83	0.67(2.31)	0.70(2)	0.99	0.88(1.72)	0.99(1)	0.94	0.79(1.98)	0.94(1)
B25-400-6-300	0.66	0.59(3.61)	0.61(3)	0.86	0.81(2.55)	0.82(2)	0.81	0.73(2.93)	0.81(1)
B25-300-10-300	0.65	0.59(3.42)	0.60(3)	0.84	0.81(2.49)	0.84(2)	0.78	0.71(2.93)	0.86(1)
B0-550-6-450	0.86	0.75(2.47)	0.78(2)	0.86	0.75(2.47)	0.78(2)	0.87	0.76(1.97)	0.87(1)
B50-0-0-0	0.73	0.73(0)	0.73(0)	0.81	0.81(0)	0.81(0)	0.80	0.80(0)	0.80(0)
B50-0-0-0R	0.86	0.86(0)	0.86(0)	0.96	0.96(0)	0.96(0)	0.95	0.95(0)	0.95(0)
B50-550-6-450	0.86	0.84(2.47)	0.86(2)	1.01	1.02(1.64)	1.05(1)	0.93	0.93(1.97)	1.00(1)
B50-450-10-450	0.87	0.84(2.30)	0.87(2)	1.04	1.08(1.60)	1.16(1)	0.93	0.94(1.97)	1.06(1)
Mean	0.82	0.76	0.78	0.95	0.91	0.94	0.92	0.87	0.95
COV	0.13	0.14	0.14	0.10	0.14	0.15	0.12	0.16	0.13

() Number of stirrups used in calculation of V_{us}.

Table 4
Summary of MC2 Model compared to experimental data.

Specimen ID	Span, l (mm)	Shear Span, a (mm)	Width, b (mm)	Depth, D (mm)	a/d_e	Longitudinal reinf. ratio, ρ_l (%)	f_{cm} (MPa)	Strut angle, θ	w_u (mm)	Tensile strength at w_u, f_w (MPa)	$\frac{V_{u,\ test}}{V_{fib\ MC2}}$
This study (MC2 Integer)											
B25-0-0-0	4500	1750	300	700	2.8	1.98	34	34.2	0.94	0.70	0.96
B25-550-6-450	4500	1750	300	700	2.8	1.98	34	34.6	1.00	0.70	1.18
B25-450-10-450	4500	1750	300	700	2.8	1.98	34	35.2	1.08	0.71	0.99
B25-400-6-300	4500	1750	300	700	2.8	1.98	46	36.1	1.21	1.09	0.82
B25-300-10-300	4500	1750	300	700	2.8	1.98	46	36.6	1.29	1.09	0.84
B50-0-0-0	4500	1750	300	700	2.8	1.98	36	36.6	1.29	1.65	0.81
B50-0-0-0R	4500	1750	300	700	2.8	1.98	36	36.6	1.29	1.65	0.96
B50-550-6-450	4500	1750	300	700	2.8	1.98	36	36.9	1.33	1.60	1.05
B50-450-10-450	4500	1750	300	700	2.8	1.98	36	37.3	1.38	1.54	1.16
Aoude et al. [14]											
A0.5%	1700	600	150	250	3.0	1.32	21.3	35.1	1.08	0.33	1.36
B0.5%	3700	1350	300	500	3.1	1.53	21.3	34.4	0.98	0.37	1.03
B1%	3700	1350	300	500	3.1	1.53	19.6	35.0	1.06	0.56	1.19
Singh and Jain [31]											
R-I	1470	875	150	300	3.5	2.67	27.8	34.6	0.99	0.88	1.13
R-II	1470	875	150	300	3.5	2.67	27.2	34.5	0.99	0.88	1.12
U-I	1470	875	150	300	3.5	2.67	27.9	34.9	1.04	1.03	1.34
U-II	1470	875	150	300	3.5	2.67	27.9	34.9	1.04	1.03	1.10
I-II	1470	875	150	300	3.5	2.67	27.1	36.3	1.24	1.67	1.26
I-II	1470	875	150	300	3.5	2.67	27.1	36.3	1.24	1.67	1.14
Minelli et al. [32]											
H1000 FRC50	5640	2820	250	1000	3.0	1.07	32.1	39.3	1.67	1.27	0.73†
H1500 FRC50	8640	4320	250	1500	3.0	1.01	32.1	39.3	1.67	1.27	0.90†
H1000 FRC75	5640	2820	250	1000	3.0	1.07	33.1	40.5	1.85	1.60	0.84††
H1500 FRC75	8640	4320	250	1500	3.0	1.01	33.1	40.6	1.86	1.59	0.99††
										Mean	1.04
										COV	0.17

† Model predicts longitudinal reinforcing steel to yield.
†† Model is limited by flexural capacity.

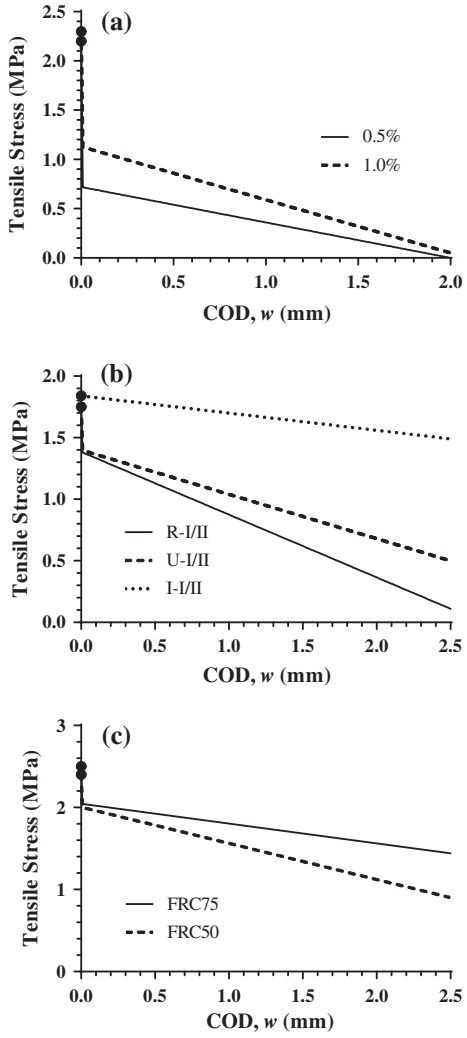

Fig. 11. Inverse analysis of prism bending tests conducted by: (a) Aoude et al. [14]; (b) Singh and Jain [31]; (c) Minelli et al. [32].

those reported by Aoude et al. [14], Singh and Jain [31] and Minelli et al. [32]. Details of the test specimens and the results are presented in Table 4. The simplified inverse analysis procedure presented in [23,29] was used to convert force–displacement data to a stress-COD resultant, with the results of the inverse analysis presented in Fig. 11.

The beam test results are compared alongside the test data of this study in Fig. 12 for the crack width corresponding to the ultimate load, the longitudinal strain measured at the specimen mid-height and the stress provided by the fibres. It can be seen that the MC2 model provides a reasonable estimation of the shear strength of SFRC beams with and without shear ligature reinforcement. It is noted that despite the reporting of the longitudinal reinforcing steel not yielding in the Minelli et al. [32] data, the MC2 model predicts the steel to reach yield for all specimens and, thus, their strength is limited by their flexural capacities.

6. Conclusions

Ten large scale SFRC beam specimens were designed, cast and tested to fail in shear. The beams were reinforced with varying dosages of steel fibres and with traditional web (ligature) reinforcement. The beams were 700 mm deep, 300 mm wide and spanned 4500 mm. Together with the beam tests, material tests (uniaxial dogbone and prism bending tests) were conducted to determine the post cracking or residual tensile strength of the SFRC.

It was demonstrated that steel fibres, if supplied in sufficient dosages, could replace the minimum amount of transverse (ligature) shear reinforcement. Although the strengths of the beams with fibres only and with the minimum amount of traditional shear ligature reinforcement were comparable, the post peak response of the specimen containing fibres only was more brittle.

It was found that for beams containing larger dosages of steel fibres, crack patterns tended to be more dispersed and cracks were visibly finer. As the load was increased towards ultimate, the cracks coalesced to form the failure crack.

A detailed comparison of design models for shear in SFRC beams from the *fib* Model Code 2010 [3] and Draft Australian Bridge Code for Concrete Structures [4] was undertaken against the test data. It was found that the alternate *fib* model (based on the work of [25]) and the Draft Australian Bridge code model provided reasonably good correlations with the test data, provided that the contribution of the ligatures is adjusted for their spacing.

The *fib* alternate model was further assessed against experimental results reported in the literature for which material data (prism bending tests) exists and the failure mode of the beams was one of shear without the longitudinal bars reaching yield [14,31,32]. It was found that the model accurately predicted the strength of the shear critical beams.

Lastly, it is noted that the 5D fibres used in the study provide high anchorage and are highly ductile. Significant benefits are likely for higher strength concrete than was adopted in this study.

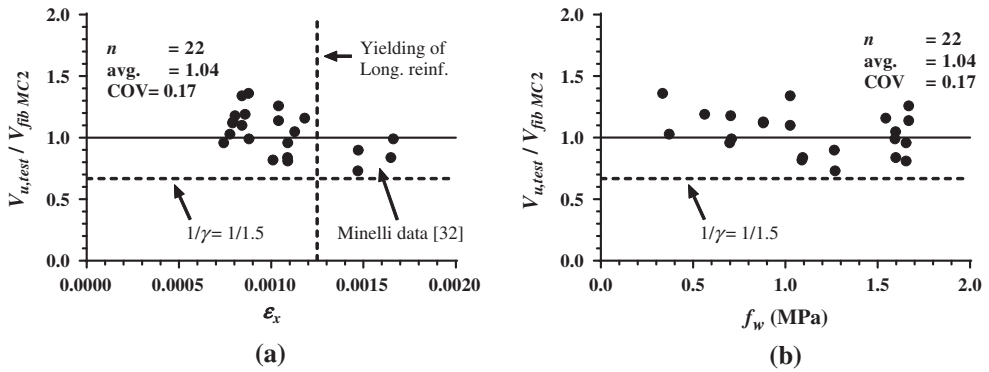

Fig. 12. Comparison of *fib* MC2 model for SFRC beams against (a) mid-height longitudinal strain parameter; (b) fibre residual tensile strength at ultimate.

Acknowledgement

The authors wish to express their gratitude to BOSFA Australia for supplying the steel fibres used in this study.

References

[1] Romualdi JP, Batson GB. Behaviour of reinforced concrete beams with closely spaced reinforcement. Proc, ACI J 1963;60(6):775–89.
[2] ACI-318. Building code requirements for structural concrete and commentary, vol. 317. ACI Committee; 2008. p. 456.
[3] *fib* Model code. Model code 2010 – final draft, vol. 1. Bulletin 65; 2012. p. 350.
[4] DR AS5100.5. Bridge design part 5: concrete. Australian Standard, Standards Association of Australia; 2014.
[5] Adebar P, Mindess S, Pierre DS, Olend B. Shear tests of fiber concrete beams without stirrups. ACI Struct J 1997;94(1):68–76.
[6] Casanova P, Rossi P, Schaller I. Can steel fibres replace transverse reinforcements in reinforced concrete beams? ACI Mater J 1997;94(5):341–54.
[7] Minelli F. Plain and fiber reinforced concrete beams under shear loading: structural behavior and design aspects. PhD dissertation. Department of Civil Engineering, University of Brescia, Italy; 2005.
[8] Voo YL, Foster SJ, Gilbert RI. Shear strength of fibre reinforced reactive powder concrete prestressed girders without stirrups. J Adv Concr Technol 2006;4(1):123–32.
[9] Dinh HH, Parra-Montesinos GJ, Wight JK. Shear behaviour of steel fiber-reinforced concrete beams without stirrup reinforcement. ACI Struct J 2010;107(5):597–606.
[10] Cuenca E. On shear behavior of structural elements made of steel fiber reinforced concrete. PhD dissertation. Universitat Politecnica de Valencia, Spain.
[11] Sahoo DR, Kumar N. Monotonic behaviour of large scale SFRC beams without stirrups. Eng Struct 2015;92:46–54.
[12] Cucchiara C, Mendola LL, Papia M. Effectiveness of stirrups and steel fibres as shear reinforcement. Cement Concr Compos 2004;26:777–86.
[13] Dancygier AN, Savir Z. Effects of steel fibres on shear behaviour of high-strength reinforced concrete beams. Adv Struct Eng 2011;14(5):745–61.
[14] Aoude H, Belghiti M, Cook WD, Mitchell D. Response of steel fiber-reinforced concrete beams with and without stirrups. ACI Struct J 2012;109(3):359–67.
[15] Spinella N, Colajanni P, La Mendola L. Nonlinear analysis of beams reinforced in shear with stirrups and steel fibres. ACI Struct J 2012;109(1):53–64.
[16] Kani GNJ. How safe are our large reinforced concrete beams? ACI J 1967;64:128–41.
[17] AS3600. Concrete structures. Australian Standard, Standards Association of Australia; 2009.
[18] Eurocode 2. Design of concrete structures – part 1–1: general rules and rules for buildings. European-Commission; 2004.
[19] Voo JYL, Foster SJ. Variable engagement model for fibre reinforced concrete in tension. UNICIV report R-420. School of Civil and Environmental Engineering, The University of New South Wales, Australia; 2003. p. 86.
[20] Voo JYL, Foster SJ. Tensile fracture of fibre reinforced concrete: variable engagement model. In: di Prisco M, Felicett R, Plizzari GA, editors. 6th Rilem symposium on fibre reinforced concrete (FRC), Varenna, Italy, 20–22 Sept; 2004. p. 875–84.
[21] CNR DT 204/2006. Guidelines for the design, construction and production control of fibre reinforced concrete structures. National Research Council of Italy; 2006.
[22] EN 14651. Test method for metallic fibre concrete-measuring the flexural tensile strength (limit of proportionality (LOP), residual). European Committee for Standardization; 2007. p. 17.
[23] Amin A, Foster SJ, Muttoni A. Derivation of the σ–w relationship for SFRC from prism bending tests. Struct Concr 2015;16:93–105.
[24] Shahnewaz M, Alam MS. Improved shear equations for steel fiber-reinforced concrete deep and slender beams. ACI Struct J 2014;111(4):851–60.
[25] Foster SJ. Design of FRC beams for shear using the VEM and the draft model code approach. *fib* Bull. 2010;57:195–210.
[26] Bentz EC, Vecchio FJ, Collins MP. The simplified MCFT for calculating the shear strength of reinforced concrete elements. ACI Struct J 2006;103(4):614–24.
[27] Foster SJ. FRC design according to the draft Australian bridge code. In: Charron JP, Massicotte B, Mobasher B, Plizzari G, editors. Proceedings FRC 2014 joint ACI-*fib* international workshop fibre reinforced concrete: from design to structural applications. Montreal, Canada, July 24–25 2014; 2014, p. 19–31.
[28] Bentz EC, Collins MP. Development of the 2004 Canadian standards association (CSA) A23.3 shear provisions for reinforced concrete. Can J Civ Eng 2006;33:521–34.
[29] Amin A, Foster SJ, Muttoni A. Evaluation of the tensile strength of SFRC as derived from inverse analysis of notched bending tests. Proceedings of the 8th international conference on fracture mechanics of concrete and concrete structures (FraMCoS-8), Toledo, Spain, 10–14 March 2013; 2013, p. 1049–57.
[30] Loov RE. Review of A23.3-94 simplified method of shear design and comparison with results using shear friction. Can J Civ Eng 1998;25:437–50.
[31] Singh B, Jain K. Appraisal of steel fibres as minimum shear reinforcement in concrete beams. ACI Struct J 2014;111(5):1191–202.
[32] Minelli F, Conforti A, Cuenca E, Plizzari G. Are steel fibres able to mitigate or eliminate size effect in shear? Mater Struct 2014;47:459–73.